

## Article

# Effect of Different Heat Treatments and Surface Treatments on the Mechanical Properties of Nickel-Titanium Rotary Files

Jihye Hong <sup>1</sup>, Sang Won Kwak <sup>1</sup> , Jung-Hong Ha <sup>2</sup> , Asgeir Sigurdsson <sup>3</sup>, Ya Shen <sup>4</sup>  and Hyeon-Cheol Kim <sup>1,\*</sup> 

<sup>1</sup> Department of Conservative Dentistry, School of Dentistry, Dental Research Institute, Dental and Life Science Institute, Pusan National University, Yangsan 50612, Republic of Korea; jihye1004zja@gmail.com (J.H.); endokwak@pusan.ac.kr (S.W.K.)

<sup>2</sup> Department of Conservative Dentistry, College of Dentistry, Kyungpook National University, Daegu 41940, Republic of Korea; endoking@knu.ac.kr

<sup>3</sup> Department of Endodontics, New York University College of Dentistry, New York, NY 10010, USA; asgeir.sigurdsson@nyu.edu

<sup>4</sup> Department of Oral Biological and Medical Sciences, Division of Endodontics, Faculty of Dentistry, University of British Columbia, Vancouver, BC V6T 1Z3, Canada; yashen@dentistry.ubc.ca

\* Correspondence: golddent@pusan.ac.kr; Tel.: +82-55-3605222

**Abstract:** This study aimed to compare the fatigue resistance of files made from different heat treatment methods and surface treatment. Four prototype files were created through heat treatment and titanium coating surface treatment (AT, DT, ER, EN; named arbitrarily by the manufacturer) at different times and temperatures. Artificial canals with curvatures of 45- and 90-degree were used for the fatigue testing. The files were operated at the speed of 500 rpm at 37 °C, and the time until fracture incurred by a 4-mm dynamic pecking motion at a speed of 8 mm/s was measured, and the number of cycles to failure (NCF) was calculated by applying rotation speed and time. The length of the fractured fragment was measured. The fractured specimens were observed under the SEM to compare the characteristics of fatigue fracture patterns. Differential scanning calorimetry analysis was performed to estimate the phase transformation temperature. One-way ANOVA with Duncan's post-hoc comparison, the Kruskal–Wallis test, and Mann–Whitney U were applied to compare the fatigue resistance among the prototypes at a significance level of 95%. Regardless of the canal angle, the EN showed the highest fatigue resistance ( $p < 0.05$ ). AT had the lowest NCF at the 90-degree canal ( $p < 0.05$ ). ER had a higher NCF than the DT at 45 degrees ( $p < 0.05$ ), but there was no difference at 90 degrees. DSC analysis revealed that the ER and EN groups exhibited two austenite peaks above 40 °C. In conclusion, the file that underwent a specific temperature heat treatment with titanium coating surface treatment showed the highest fatigue resistance.

**Keywords:** nickel-titanium file; fatigue; fracture resistance; heat treatment; surface treatment



**Citation:** Hong, J.; Kwak, S.W.; Ha, J.-H.; Sigurdsson, A.; Shen, Y.; Kim, H.-C. Effect of Different Heat Treatments and Surface Treatments on the Mechanical Properties of Nickel-Titanium Rotary Files. *Metals* **2023**, *13*, 1769. <https://doi.org/10.3390/met13101769>

Academic Editors: Xudong Qian, Zhiqiang Liang and Lijing Xie

Received: 29 August 2023

Revised: 3 October 2023

Accepted: 17 October 2023

Published: 18 October 2023



**Copyright:** © 2023 by the authors. Licensee MDPI, Basel, Switzerland. This article is an open access article distributed under the terms and conditions of the Creative Commons Attribution (CC BY) license (<https://creativecommons.org/licenses/by/4.0/>).

## 1. Introduction

The successful performance of root canal treatment requires technical expertise and precision. To achieve this, clinicians carefully manipulate hand files within the root canal space while adhering to essential principles for disinfection and treatment. Traditionally, stainless steel files were used to form an appropriate root canal shape using various manipulation techniques [1,2].

However, the introduction of nickel-titanium (NiTi) files in the late 1980s revolutionized root canal treatment technology, as they showed significant advantages over stainless-steel files in terms of instrument stability [1]. NiTi files are more flexible for filing, reaming, turn-and-full, and balanced force techniques. They also offer a shorter shaping time and are less prone to procedural errors, such as zip, ledge, or transportation, due to their super-elasticity [1,2]. NiTi files maintain the original canal shape during preparation, and furthermore, the super-elasticity of the NiTi rotating file can create a desirable

root canal shape with a significantly reduced canal transportation tendency in clinical practice [3–9]. With these advantages, the use of the NiTi file has increased significantly since its introduction and NiTi instruments are generally being used nowadays in root canal treatment.

During the last 20 years, despite considerable advances in file design and manufacturing procedures, fracturing of the NiTi instrument caused by torsion or cyclic fatigue is still a problem, especially in calcified or severely curved root canals [7–10]. Previous studies have shown that the types of fractures in the NiTi instrument are mainly cyclic bending or torsional twisting [9,10]. Cyclic bending fatigue occurs when the instrument rotates in a curved canal, which creates repeated compressive and tensile stresses. Meanwhile, a torsional failure occurs when the tip of the instrument is coupled to the canal while the motor continues to rotate [7,10].

Manufacturers are trying to solve these problems and develop NiTi files with superior mechanical properties through heat treatment, surface treatment, various cross-sectional designs, and new manufacturing processes [11–13].

Meanwhile, the concept of minimally invasive procedures has been introduced recently and applied to practical dentistry [14]. Minimally invasive treatment has also increased the conservation of tooth structure material for better prognosis of endodontically treated teeth (ETT) [15]. Minimally invasive access was reported to preserve coronal dentin and increase the fracture resistance of ETT [15,16].

Recently, some NiTi file systems in the form of smaller tapers and thinner shafts were introduced to preserve peri-cervical dentin and consequently improve the prognosis of ETT. It has been suggested that minimally invasive root canal preparation performed using NiTi files with a smaller taper may better preserve the root dentin tissue compared to using larger-tapered NiTi files, thus increasing the fracture resistance of ETT [17,18].

One of the most representative minimally invasive file systems is the TruNatomy system (Dentsply Sirona, Ballaigues, Switzerland). TruNatomy is a newly released file system made from 0.8 mm NiTi wires, which is smaller than the 1.2 mm NiTi wires commonly used to manufacture most files. It also undergoes special heat treatment. TruNatomy asserts improved resistance to cyclic fatigue and reduced risk of file separation [19,20].

Another file system based on the minimally invasive concept has been developed by a manufacturing company (Maruchi, Wonju, Republic of Korea). During the development process, various heat treatments and surface treatments were attempted to enhance the mechanical properties of the thin file system, aiming to achieve higher fracture resistance.

The purpose of this study was to compare the fatigue fracture resistance of the prototype files with different heat treatments and surface treatments (Memory-Triple (MT) technology) while using files of the same size and shape. The null hypothesis was that all prototypes have the same fatigue fracture resistance.

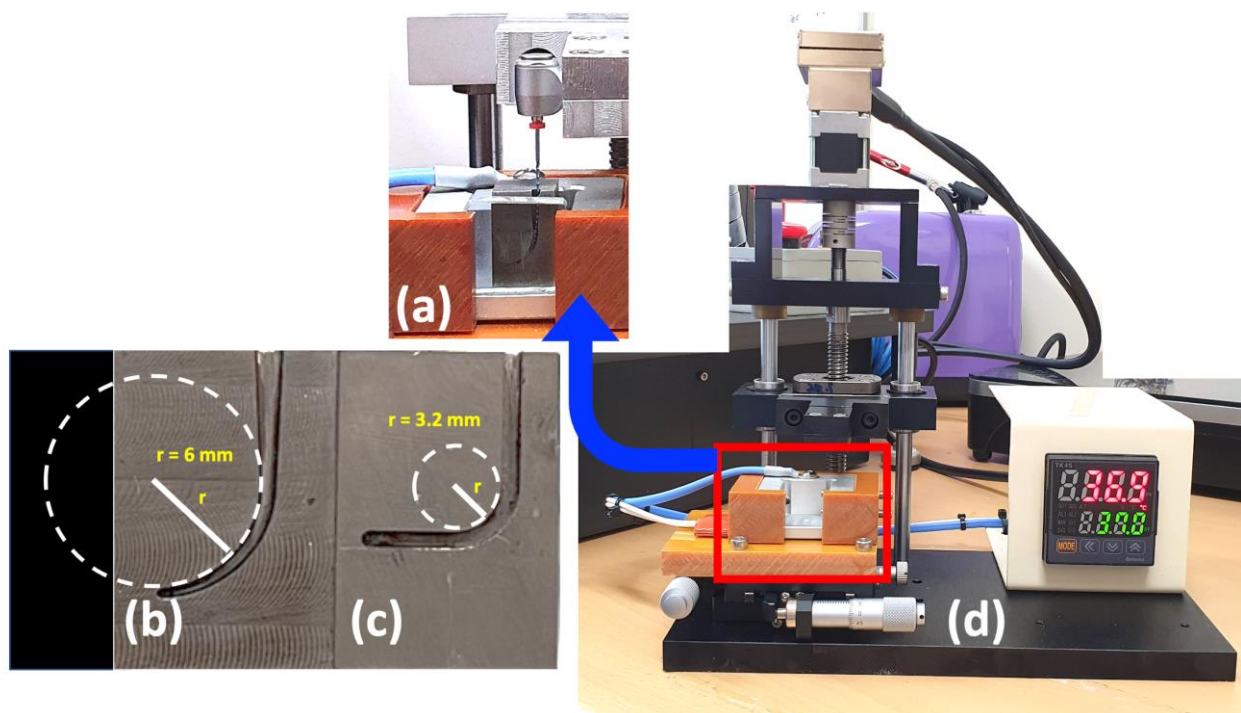
## 2. Materials and Methods

In order to compare fatigue fracture resistances by heat treatments and surface treatments of the same files, four types of prototype files were manufactured by the Maruchi Company. Four different types of prototypes were named arbitrarily by the manufacturer as AT, DT, ER, and EN, respectively. They were made by different courses of heat treatment and surface titanium coating (Table 1).

All the files used in this experiment were 25 mm long and had tip sizes of #25/04. G\*Power v3.1 (Heinrich Heine University Düsseldorf Universität, Düsseldorf, Germany) was used to determine the appropriate sample size for the tests with a 5% level of significance and a test power of 0.80. A total of 104 files were used for the fatigue fracture experiments. They were divided into two groups based on the curvatures of simulated canals: 45 degrees with a 6 mm radius and 90 degrees with an approximately 3.2 mm radius, as measured using the method described by Schneider [21]. These artificial canal blocks were made of tempered steel (Figure 1).

**Table 1.** Main conditions and order (1, 2, 3, and/or 4) of the Memory-Triple (MT) technology for the tested groups (courtesy of the Maruchi company).

Group	Heat Treatment Temperature	Titanium Coating	Note
AT	1. 500 °C 2. 400 °C 4. 500 °C	3. Yes	mainly Austenite at body temperature
DT	1. 500 °C 2. 400 °C 4. 500 °C (30 s) > Cooling (15 °C)	3. Yes	similar ratio of Austenite and Martensite
ER	1. 500 °C 2. 400 °C 3. 320 °C	No	mainly Martensite at body temperature
EN	1. 500 °C 2. 400 °C 4. 320 °C	3. Yes	

**Figure 1.** The test device (EndoC: DMJ system, Busan, Republic of Korea) used in this study for the cyclic fatigue test. (a) Simulated canal in the heat generation pad (detailed from red box), (b) 45-degree canal curvature with a 6 mm radius, (c) 90-degree canal curvature with a 3.2 mm radius, (d) Electronic heat controller.

The cyclic fatigue fracture resistance tests were conducted using a custom-made device (EndoC; DMJ systems, Busan, Republic of Korea) (Figure 1). The artificial canal block was located in this device and the block was heated with a thermal control element that adjusts the temperature to 37 °C. An X-Smart Plus motor (Dentsply Sirona) was connected to the device, and the rotation speed of the motor was set to 500 rpm according to the manufacturer's instructions. Each NiTi file from the four groups ( $n = 13$ ) was rotated with a repetitive up-and-down movement in the curved canal with 4 mm of pecking distance inside the 17 mm length of the simulated canal.

The time when the file tip breaks was measured audibly and visibly. The number of cycles to failure (NCF) was calculated by applying the rotation speed and time (seconds) to

fracture. The length of the fractured fragment was measured using a digital microcaliper (Mitutoyo, Kanagawa, Japan).

To evaluate the data and compare the file subgroups, the statistics program SPSS (version 25.0; SPSS Inc., Chicago, IL, USA) was used. The Levene test was used to evaluate the normality of the continuous results. Under the conditions of normal distribution, one-way analysis of variance (ANOVA) and Duncan post-hoc comparison were applied to compare the prototypes. In case the data did not show normal distributions, data were compared using the Kruskal–Wallis test and Mann–Whitney U test. In all experiments, a  $p$ -value of less than 0.05 was considered significant.

### 2.1. Differential Scanning Calorimetry

Differential scanning calorimetry (DSC) analysis was performed to estimate austenite phase transformation temperatures. DSC technology measures the amount of heat emitted or absorbed by a small sample when an alloy is cooled or heated through phase transformation to produce a thermogram with a characteristic peak [22]. Based on previous tests conducted in our laboratory, the maximum temperature (80 °C) during calorimetric heating was determined to be sufficiently above the temperature required to achieve a fully austenite state for each of the examined specimens [23,24]. DSC measures the temperatures and heat flows associated with transitions in materials as a function of time and temperature in a controlled atmosphere. Five specimens from each prototype were chosen for DSC analysis (DSC Q2000 V24.4 Build 116, TA Instruments, New Castle, DE, USA). The heating and cooling curves were automatically acquired by the device to observe changes in the phase transition start temperature and enthalpy. Based on the DSC profiles, the onset and completion temperatures of each phase transformation were established by identifying the points where the tangents to a thermal peak intersected with a baseline. Following the widely accepted convention, this paper expresses these temperatures as  $M_s$ ,  $M_f$ ,  $A_s$ , and  $A_f$ , representing the starting and finishing temperatures of the martensite, and austenite, respectively [25–27]. These transition temperatures indicate at what stage each NiTi instrument is present under the experimental temperature conditions.

### 2.2. Scanning Electronic Microscopic Analysis

After the cyclic fatigue fracture tests, 5 fractured fragments from each group were observed using scanning electron microscopy (SEM; JSM-7200F, JEO, Tokyo, Japan) to evaluate the topographic features of the fractured surfaces at the cross-sections and longitudinal aspects.

## 3. Results

Using descriptive statistics, the average and standard deviation results of the four groups of files are shown in Table 2. In the Levene test, a normal distribution was achieved, and the ANOVA test with Duncan post-hoc comparison was conducted for the NCF in the simulated 45-degree canal with fragment lengths in both canal curvature conditions. Data from the 90-degree NCF were compared using the Kruskal–Wallis test and Mann–Whitney U test.

The EN group showed the highest NCF of fatigue resistance in both canal conditions compared to other groups ( $p < 0.05$ ). The AT group showed the least NCF in both canal conditions compared to the others ( $p < 0.05$ ). ER had a higher NCF than DT in the 45-degree canal ( $p < 0.05$ ) but there were no differences between groups in the 90-degree canal.

The fracture fragment did not show differences but the AT groups showed longer lengths than other groups in the 45-degree canal ( $p < 0.05$ ).

The DSC analysis showed all groups had different features of austenite phase transformation temperatures (Figure 2). The AT groups had austenite finishing temperatures ( $A_f$ ) around body temperature. The ER and EN groups show two peaks of austenite finishing temperature ( $A_f$ ) at temperatures over 40 °C.

**Table 2.** Cyclic fatigue fracture resistances (NCF: number of cycles to failure) of the 4 groups of prototypes and fracture length (mm) in two conditions of canal curvatures.

Group	45-Degree		90-Degree	
	NCF	Fragment Length	NCF *	Fragment Length
AT	1042 ± 231 <sup>c</sup>	5.03 ± 0.63 <sup>a</sup>	613 ± 100 <sup>c</sup>	4.83 ± 0.73
DT	1212 ± 204 <sup>c</sup>	4.37 ± 0.33 <sup>b</sup>	804 ± 78 <sup>b</sup>	4.91 ± 0.66
ER	2083 ± 458 <sup>b</sup>	4.53 ± 0.47 <sup>b</sup>	861 ± 230 <sup>b</sup>	4.59 ± 0.97
EN	2357 ± 257 <sup>a</sup>	4.58 ± 0.57 <sup>b</sup>	1062 ± 150 <sup>a</sup>	4.92 ± 0.74

\*: NCF in the curvature of 90 degrees was compared using the Kruskal–Wallis test and Mann–Whitney U test. Others were compared using the ANOVA test with Duncan post-hoc comparison. <sup>a,b,c</sup>: Different superscript alphabets represent significant differences between groups ( $p < 0.05$ ).

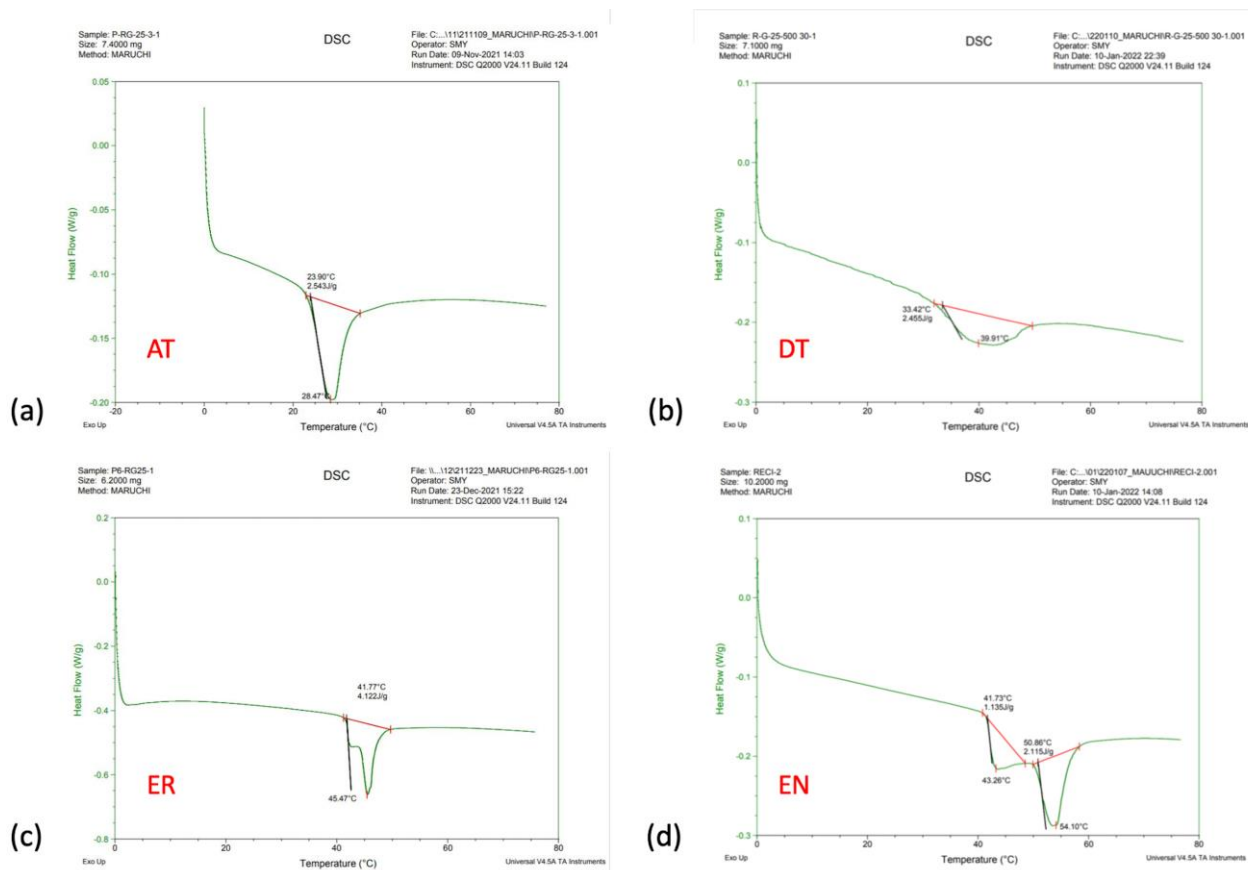


**Figure 2.** Representative differential scanning calorimetry (DSC) graphs. (a) AT group had the austenite finishing (Af) temperature around body temperature. AT group showed the martensite finishing (Mf) at around 23 °C. (b) DT group had austenite start (As) temperature at around 33 °C and austenite peak (Ap) temperature at around 40 °C. (c) ER and (d) EN groups had As temperature over 40 °C of temperature and showed two peaks of austenite. ER and EN groups had files in martensite until they reached 40 °C.

SEM examination showed the files from the four groups had similar topographic features of cyclic fatigue fracture. Typical features of cyclic fatigue fracture including microcracks in the longitudinal aspects (Figure 3), crack initiation area, and fatigue fracture zone in the cross-sections (Figure 4) were found. There were no different topographic features from the different angles of canal curvature.

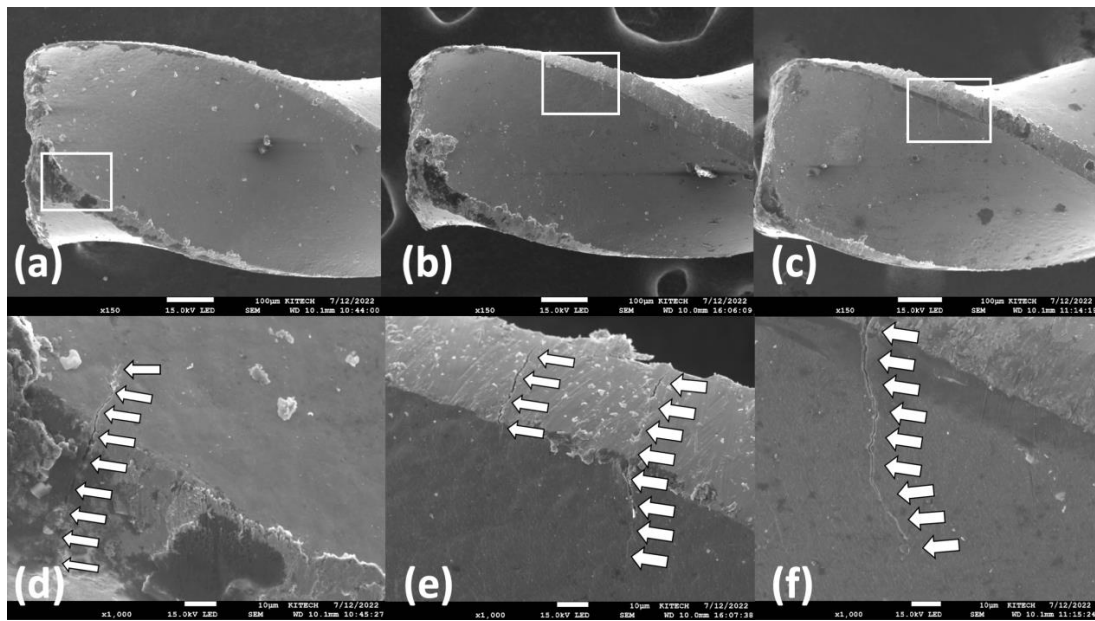


**Figure 3.** Representative scanning electron micrographs (a–c):  $\times 150$  magnification, (d–f):  $\times 1000$  magnification) of the fracture surface of fractured fragments after the cyclic fatigue tests ((a,d): DT, (b,e): ER, (c,f): EN). Longitudinal aspects show typical aspects of cyclic fatigue fracture. White arrows in the magnified ( $\times 1000$ ) views show microcracks near the fracture area. White rectangular boxes (a–c) were magnified to (d–f), respectively. No specific differences were found according to the groups.

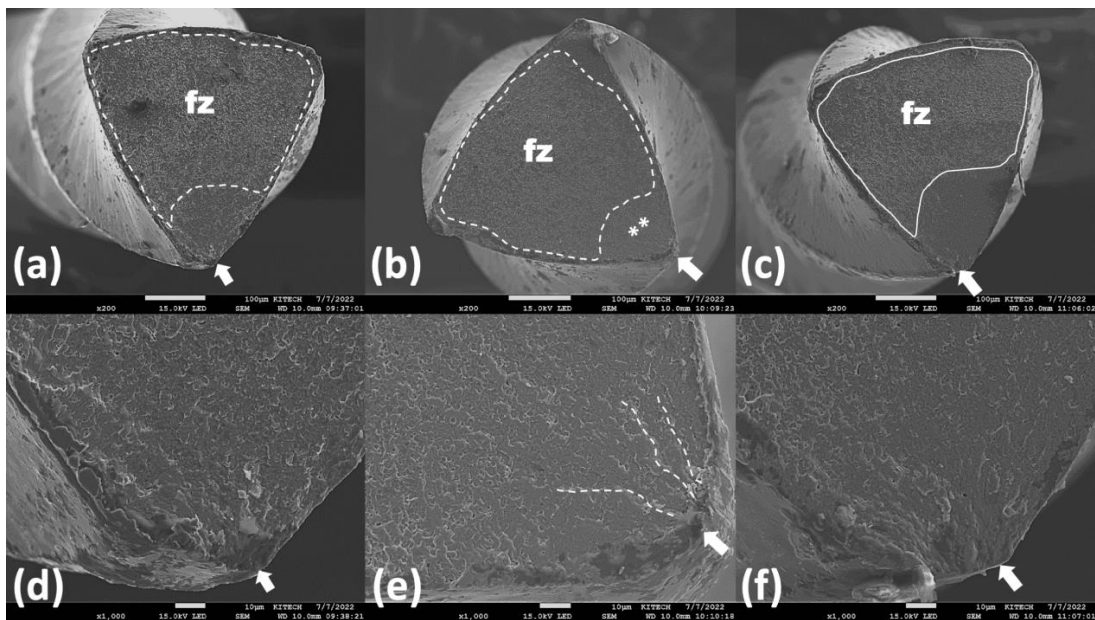


**Figure 4.** Representative scanning electron micrographs (a–c):  $\times 150$  magnification, (d–f):  $\times 1000$  magnification) of the fracture surface of fractured fragments after the cyclic fatigue tests ((a,d): AT, (b,e): DT, (c,f): EN). All specimens show similar topographic features regardless of the groups. Cross-sectional aspects show typical aspects of cyclic fatigue fracture including crack initiation area (white arrows) and fatigue fracture zone (fz). Most of the specimens show big areas (outlined with a dotted line) of fatigue fracture zones (fz) with numerous ductile dimples in the opposite area of the crack initiation area. (b,e) Some specimens show the crack propagation in river-flow-like striations (asterisk and dotted line). No specific differences were found according to the groups.

Lateral aspects showed highly polished surfaces without machining grooves (Figure 3a–c;  $\times 150$  magnification). Therefore, the microcracks were not straight and ran in irregular (arrows indicated) shapes (Figure 3d–f;  $\times 1000$  magnification).

Cross-sectional aspects (Figure 4) show typical aspects of cyclic fatigue fracture including the crack initiation area (white arrows) and fatigue fracture zone (fz). All specimens show similar topographic features regardless of group. The typical feature of the “overload fast fracture zone” could be observed at the opposite side of the crack initiation area. Some specimens show the crack propagation in river-flow-like striations (Figure 4e, dot line).

#### 4. Discussion

Despite various efforts to reduce the occurrence of fractures in NiTi files, fractures can still occur unexpectedly during the endodontic treatment process [27–29]. If a separated fragment of the NiTi file cannot be removed from the root canal due to fracture, it can have a negative impact on the clinical prognosis as effective removal of infected pulp or bacteria may not be possible [27,28].

Manufacturers have undertaken extensive efforts to address these challenges and develop NiTi files with better fracture resistance and efficient clinical performance. Many heat treatment technologies for NiTi alloys have been introduced; R-phase, M-wire, CM-wire, T-wire, Gold-wire, Blue-wire, etc [11–13,29–31].

R-phase heat treatment technology (SybronEndo, Glendora, CA, USA) was employed to produce improved NiTi alloys. The K3XF file (SybronEndo) was released using R-phase heat treatment [29,30]. By using R-phase heat treatment after the grinding process, the alloy is deformed into a slightly different crystal structure. According to the manufacturer, the new thermal process provides equipment with greater flexibility and resistance to periodic fatigue than files made from traditional NiTi alloys [29,30]. The manufacturer also used R-phase heat treatment to twist (instead of grinding) NiTi wires to develop the Twisted File. The manufacturer promoted excellent flexibility and cyclic fatigue resistance [29,30].

With the manufacturing technology established to develop M-wire NiTi focusing on metallography, this technology uses heat treatment to improve periodic fatigue resistance and device flexibility [31]. Typical files made of M-wire include WaveOne (Dentsply Sirona, Ballaigues, Switzerland), Reciproc (VDW, Munich, Germany), original reciprocating file systems, etc. [32]. As one of them, ProTaper Next (Dentsply Sirona) is also an M-wire rotary file system produced by heat treatment that has been reported to improve flexibility and fatigue resistance [33].

Another novel type of NiTi rotary instrument, manufactured from controlled memory wire (CM-wire; DS Dental, Johnson City, TN, USA), has been introduced. In conventional NiTi alloys, when subjected to a specific range of mechanical loads, the austenite phase undergoes a transformation into stress-induced martensite [33]. However, the martensite phase is inherently unstable at temperatures above the austenite finishing ( $A_f$ ) temperature and reverts back to austenite upon removal of the load. Consequently, the  $A_f$  of conventional super-elastic NiTi files should be below the working temperature. Nevertheless, the utilization of CM-wire technology enables NiTi files to eliminate the rebound effect following unloading, as they can regain their original shape through heat application or autoclaving procedures. This behavior can be attributed to the presence of a stable martensite phase, indicating that the  $A_f$  is above the working temperature [34]. According to the manufacturer and previous studies, CM-wire instruments are purported to possess superior flexibility and resistance to cyclic fatigue compared to conventional NiTi files. However, a separate study indicated that the ultimate tensile strength of CM-wire instruments was lower than that of conventional super-elastic NiTi wires [34,35].

T-wire heat treatment, introduced by the company Micro-Mega (Micro-Mega, Besançon, France) was used in the manufacture of the OneFlare (Micro-Mega) and 2Shape (Micro-Mega) file systems. By exposure to T-wire heat treatment after the grinding process, the traditional microstructure of the NiTi alloy undergoes slight changes, resulting in the instrument having higher fatigue resistance and increased flexibility [36,37]. The 2Shape

(Micro-Mega) instrument is a new group of endodontic file systems that uses T-wire technology to enhance the cyclic fatigue resistance of endodontic instruments by 40%, along with the flexibility of the files [36,37].

Gold-wire and Blue-wire have also been applied to many brands' file systems as martensite-dominant files recently; ProTaper Gold, Reciproc Blue (VDW), EdgeTaper (EdgeEndo, Albuquerque, NM, USA), etc. The ProTaper Ultimate system (Dentsply Sirona) includes various heat-treated files in the single system that incorporate M-wire, Gold-wire, and Blue-wire.

The concept of minimally invasive procedures has been introduced and applied to various practical dentistry [14–16]. Minimally invasive approaches to endodontics have gained popularity for preserving tooth structure and enhancing the prognosis of ETT [15,16]. Some NiTi file systems in the form of smaller tapers and thinner shafts were introduced to preserve peri-cervical dentin and, consequently, improve the prognosis of ETT [21–23]. The TruNatomy system, one notable minimally invasive file system, was reported to have increased cyclic fatigue resistance using a thin-shaft and heat-treated alloy [20]. Reddy et al. [38] reported that the TN system had better fatigue resistance than the ProTaper Gold system, made of a gold alloy, although Elnaghy et al. [39] reported that TN showed a lower fatigue resistance than the HyFlex CM instruments (DS Dental) made of CM-wire [19,38,39]. These findings might result from the difference in heat treatment as well as the geometric characteristics [35].

The company Maruchi tried to develop another file system comparable to TruNatomy using MT technology along with heat treatment and surface treatment. This study compared fatigue fracture resistances using the prototype files with different heat treatments and surface treatments while using files of the same size and shape.

When comparing NCF and length, it is evident from Table 2 that NCF is much higher at 45 degrees than at 90 degrees. This implies that the likelihood of file fracture is higher with increased root curvature. The lengths of the broken pieces do not show a significant difference between 45- and 90-degree canal curvatures. The AT file, which exhibited the lowest NCF and fractured slightly later than the other groups at 45 °C, was treated with a titanium coating but was heated to a higher temperature (500 °C) compared to the ER and EN files (320 °C) and did not undergo cooling in the fourth heating process. As a result, austenite started at 23 °C and peaked at around body temperature (approximately 37 degrees). This means that even with a titanium coating, if the heating and cooling process is excessively high, austenite in the file occurs more quickly, resulting in faster breakage. When comparing ER and EN, which showed slightly higher NCF, they were treated at the same temperature and showed a peak in austenite at 40 °C. Until then, the two files were in a martensite state. This means that the file's flexibility can be maintained for a longer period of time at high temperatures, resulting in delayed fracture. When comparing EN, which showed the highest NCF, with ER, EN was treated with a titanium coating, while ER did not undergo surface treatment.

The manufacturer states that the thickness of the titanium coating is approximately 100 nanometers (0.1 micrometer) based on the transmission electron microscopy (TEM) analysis. The role of the coating would be presumed to eliminate the machining defects during file manufacturing, distribute stress on files during root canal enlargement, and compensate for bending stress in files. The affect from the surface coating might have made the file have stable resistance. Based on the results (Table 2), the ER group which had the same heat treatment as the EN group had much greater standard deviation (compared to the mean value), resulting in data without normal distribution. From this, we could also estimate that the surface coating increased the stability of the fracture resistance.

The changes in material properties resulting from heat treatment have a significant impact on the mechanical characteristics and improve the clinical performance compared to files of the same design and size made with conventional NiTi alloys [36].

The present study suggests that heat and surface treatments are highly promising methods for enhancing the efficiency and safety of modern endodontic instruments. The

EN group in this study was commercially launched as a brand file (EndoRoad) from the Maruchi company and the company presented their technique as a new heat treatment using MT technology. However, it is important to note that all file systems have its own advantages and disadvantages, and the properties are determined by various factors such as alloy type by heat treatment, degree of taper, and cross-sectional design.

## 5. Conclusions

In conclusion, among the heat treatment methods attempted during the manufacturing process by the Maruchi company, the EN group showed the highest NCF of fatigue resistances in both canal conditions with different curvature angles and radii. Conclusively, the EN group that underwent Memory-Triple heat treatment along with titanium coating surface treatment exhibited the highest fatigue fracture resistance.

Considering the limitations of the laboratory experimental study conducted, the presented results can provide valuable insights for the manufacturing of NiTi files. It is necessary to apply and evaluate the method that demonstrated the highest fracture resistance on other files in order to expand its application.

**Author Contributions:** Conceptualization, H.-C.K. and S.W.K.; methodology, J.H.; software, J.-H.H.; validation, A.S., Y.S. and H.-C.K.; formal analysis, J.H.; investigation, S.W.K.; resources, J.-H.H.; data curation, J.H.; writing—original draft preparation, J.H.; writing—review and editing, Y.S. and A.S.; visualization, S.W.K.; supervision, Y.S. and H.-C.K.; project administration, H.-C.K. All authors have read and agreed to the published version of the manuscript.

**Funding:** This research received no external funding.

**Data Availability Statement:** All data included in this study are available from the corresponding author on reasonable request.

**Acknowledgments:** All listed authors have contributed significantly to this study/manuscript and are in agreement with the manuscript. Jihye Hong and Sang Won Kwak contributed equally to this work and share the first authorship.

**Conflicts of Interest:** The authors declare no conflict of interest.

## References

1. Walia, H.M.; Brantley, W.A.; Gerstein, H. An initial investigation of the bending and torsional properties of Nitinol root canal files. *J. Endod.* **1988**, *14*, 346–351. [[CrossRef](#)] [[PubMed](#)]
2. Liu, S.B.; Fan, B.; Cheung, G.S.; Peng, B.; Fan, M.W.; Gutmann, J.L.; Song, Y.L.; Fu, Q.; Bian, Z. Cleaning effectiveness and shaping ability of rotary ProTaper compared with rotary GT and manual K-Flexofile. *Am. J. Dent.* **2006**, *19*, 353–358. [[PubMed](#)]
3. Peters, O.A. Current challenges and concepts in the preparation of root canal systems: A review. *J. Endod.* **2004**, *30*, 559–567. [[CrossRef](#)] [[PubMed](#)]
4. Schäfer, E.; Schulz-Bongert, U.; Tulus, G. Comparison of hand stainless steel and nickel titanium rotary instrumentation: A clinical study. *J. Endod.* **2004**, *30*, 432–435. [[CrossRef](#)] [[PubMed](#)]
5. Chen, J.L.; Messer, H.H. A comparison of stainless steel hand and rotary nickel-titanium instrumentation using a silicone impression technique. *Aust. Dent. J.* **2002**, *47*, 12–20. [[CrossRef](#)]
6. Pettiette, M.T.; Delano, E.O.; Trope, M. Evaluation of success rate of endodontic treatment performed by students with stainless-steel K-files and nickel-titanium hand files. *J. Endod.* **2001**, *27*, 124–127. [[CrossRef](#)]
7. Sattapan, B.; Nervo, G.J.; Palamara, J.E.; Messer, H.H. Defects in rotary nickel-titanium files after clinical use. *J. Endod.* **2000**, *26*, 161–165. [[CrossRef](#)]
8. Cheung, G.S.; Peng, B.; Bian, Z.; Shen, Y.; Darvell, B.W. Defects in ProTaper S1 instruments after clinical use: Fractographic examination. *Int. Endod. J.* **2005**, *38*, 802–809. [[CrossRef](#)]
9. Shen, Y.; Cheung, G.S.; Peng, B.; Haapasalo, M. Defects in nickel-titanium instruments after clinical use. Part 2: Fractographic analysis of fractured surface in a cohort study. *J. Endod.* **2009**, *35*, 133–136. [[CrossRef](#)]
10. Kramkowski, T.R.; Bahcall, J. An in vitro comparison of torsional stress and cyclic fatigue resistance of ProFile GT and ProFile GT Series X rotary nickel-titanium files. *J. Endod.* **2009**, *35*, 404–407. [[CrossRef](#)]
11. Lopes, H.P.; Gambarra-Soares, T.; Elias, C.N.; Siqueira, J.F., Jr.; Inojosa, I.F.; Lopes, W.S.; Vieira, V.T. Comparison of the mechanical properties of rotary instruments made of conventional nickel-titanium wire, M-wire, or nickel-titanium alloy in R-phase. *J. Endod.* **2013**, *39*, 516–520. [[CrossRef](#)] [[PubMed](#)]

12. Shen, Y.; Qian, W.; Abtin, H.; Gao, Y.; Haapasalo, M. Fatigue testing of controlled memory wire nickel-titanium rotary instruments. *J. Endod.* **2011**, *37*, 997–1001. [[CrossRef](#)] [[PubMed](#)]
13. Pedullà, E.; Lo Savio, F.; Boninelli, S.; Plotino, G.; Grande, N.M.; La Rosa, G.; Rapisarda, E. Torsional and cyclic fatigue resistance of a new nickel-titanium instrument manufactured by electrical discharge machining. *J. Endod.* **2016**, *42*, 156–159. [[CrossRef](#)] [[PubMed](#)]
14. Shabbir, J.; Zehra, T.; Najmi, N.; Hasan, A.; Naz, M.; Piasecki, L.; Azim, A.A. Access cavity preparations: Classification and literature review of traditional and minimally invasive endodontic access cavity designs. *J. Endod.* **2021**, *47*, 1229–1244. [[CrossRef](#)] [[PubMed](#)]
15. Barbosa, A.F.A.; Lima, C.O.; Sarmiento, E.B.; Cunha, G.G.D.; Sassone, L.M.; Lopes, R.T.; Nogueira Leal da Silva, E.J. Impact of Minimally Invasive Endodontic Procedures on the Development of Dentinal Microcracks. *J. Endod.* **2022**, *48*, 1146–1151. [[CrossRef](#)]
16. Zhang, Y.; Liu, Y.; She, Y.; Liang, Y.; Xu, F.; Fang, C. The effect of endodontic access cavities on fracture resistance of first maxillary molar using the extended finite element method. *J. Endod.* **2019**, *45*, 316–321. [[CrossRef](#)]
17. Zinge, P.R.; Patil, J. Comparative evaluation of effect of rotary and reciprocating single-file systems on pericervical dentin: A cone-beam computed tomography study. *J. Conserv. Dent.* **2017**, *20*, 424–428. [[CrossRef](#)]
18. Jiang, Q.; Huang, Y.; Tu, X.; Li, Z.; He, Y.; Yang, X. Biomechanical properties of first maxillary molars with different endodontic cavities: A finite element analysis. *J. Endod.* **2018**, *44*, 1283–1288. [[CrossRef](#)]
19. Silva, E.J.N.L.; Lima, C.O.; Barbosa, A.F.A.; Lopes, R.T.; Sassone, L.M.; Versiani, M.A. The impact of TruNatomy and ProTaper Gold instruments on the preservation of the periradicular dentin and on the enlargement of the apical canal of mandibular molars. *J. Endod.* **2022**, *48*, 650–658. [[CrossRef](#)]
20. The TruNatomy, Brochure, Ballaigues, Switzerland, Dentsply Sirona. Available online: [http://www.henryschein.nl/images/assets/TruNatomy\\_Brochure\\_LR%20EN%200219.pdf](http://www.henryschein.nl/images/assets/TruNatomy_Brochure_LR%20EN%200219.pdf) (accessed on 1 March 2023).
21. Schneider, S.W. A comparison of canal preparations in straight and curved root canals. *Oral Surg. Oral Med. Oral Pathol.* **1971**, *32*, 271–275. [[CrossRef](#)]
22. Measuring Transformation Temperatures in Nitinol Alloys, Johnson Matthey Medical. Available online: <http://jmmedical.com/resources.html> (accessed on 1 March 2023).
23. Kus, K.; Breczko, T. DSC-investigations of the effect of annealing temperature on the phase transformation behavior in Ni-Ti shape memory alloy. *Mater. Phys. Mech.* **2010**, *9*, 75–83.
24. Tang, W.; Sandström, R.; Wei, Z.G.; Miyazaki, S. Experimental investigation and thermodynamic calculation of the Ti-Ni-Cu shape memory alloys. *Metall. Mater. Trans. A* **2000**, *31*, 2423–2430. [[CrossRef](#)]
25. ASTM F 2004-17; Standard Test Method for Transformation Temperature of Nickel-Titanium Alloys by Thermal Analysis. American Society for Testing and Materials: West Conshohocken, PA, USA, 2016.
26. ASTM E967-18; Standard Test Method for Temperature Calibration of Differential Scanning Calorimeters and Differential Thermal Analyzers. American Society for Testing and Materials: West Conshohocken, PA, USA, 2018.
27. Shen, Y.; Zhou, H.M.; Zheng, Y.F.; Peng, B.; Haapasalo, M. Current challenges and concepts of the thermomechanical treatment of nickel-titanium instruments. *J. Endod.* **2013**, *39*, 163–172. [[CrossRef](#)] [[PubMed](#)]
28. Glossen, C.R.; Haller, R.H.; Dove, S.B.; del Rio, C.E. A comparison of root canal preparations using Ni-Ti hand, Ni-Ti engine-driven, and K-Flex endodontic instruments. *J. Endod.* **1995**, *21*, 146–151. [[CrossRef](#)]
29. Ha, J.H.; Kim, S.K.; Cohenca, N.; Kim, H.C. Effect of R-phase heat treatment on torsional resistance and cyclic fatigue fracture. *J. Endod.* **2013**, *39*, 389–393. [[CrossRef](#)]
30. Kim, H.C.; Yum, J.; Hur, B.; Cheung, G.S. Cyclic fatigue and fracture characteristics of ground and twisted nickel-titanium rotary files. *J. Endod.* **2010**, *36*, 147–152. [[CrossRef](#)]
31. Ye, J.; Gao, Y. Metallurgical characterization of M-wire nickel-titanium shape memory alloy used for endodontic rotary instruments during low-cycle fatigue. *J. Endod.* **2012**, *38*, 105–107. [[CrossRef](#)]
32. Özyürek, T. Cyclic Fatigue Resistance of Reciproc, WaveOne, and WaveOne Gold Nickel-Titanium Instruments. *J. Endod.* **2016**, *42*, 1536–1539. [[CrossRef](#)]
33. Capar, I.D.; Arslan, H.; Akcay, M.; Uysal, B. Effects of ProTaper Universal, ProTaper Next, and HyFlex instruments on crack formation in dentin. *J. Endod.* **2014**, *40*, 1482–1484. [[CrossRef](#)]
34. de Arruda Santos, A.; de Azevedo Bahia, M.G.; de Las Casas, E.B.; Buono, V.T. Comparison of the mechanical behavior between controlled memory and superelastic nickel-titanium files via finite element analysis. *J. Endod.* **2013**, *39*, 1444–1447. [[CrossRef](#)]
35. Goo, H.J.; Kwak, S.W.; Ha, J.H.; Pedullà, E.; Kim, H.C. Mechanical properties of various heat-treated nickel-titanium rotary instruments. *J. Endod.* **2017**, *43*, 1872–1877. [[CrossRef](#)] [[PubMed](#)]
36. Ataya, M.; Ha, J.H.; Kwak, S.W.; Abu-Tahun, I.H.; El Abed, R.; Kim, H.C. Mechanical properties of orifice preflaring nickel-titanium rotary instrument heat treated using T-wire technology. *J. Endod.* **2018**, *44*, 1867–1871. [[CrossRef](#)]
37. Pedullà, E.; Canova, F.S.; La Rosa, G.R.M.; Naaman, A.; Diemer, F.; Generali, L.; Nehme, W. Influence of NiTi Wire Diameter on Cyclic and Torsional Fatigue Resistance of Different Heat-Treated Endodontic Instruments. *Materials* **2022**, *15*, 6568. [[CrossRef](#)] [[PubMed](#)]

38. Reddy, B.N.; Murugesan, S.; Basheer, S.N.; Kumar, R.; Kumar, V.; Selvaraj, S. Comparison of Cyclic Fatigue Resistance of Novel TruNatomy Files with Conventional Endodontic Files: An In Vitro SEM Study. *J. Contemp. Dent. Pract.* **2021**, *22*, 1243–1249. [[PubMed](#)]
39. Elnaghy, A.M.; Elsaka, S.E.; Elshazli, A.H. Dynamic cyclic and torsional fatigue resistance of TruNatomy compared with different nickel-titanium rotary instruments. *Aust. Endod. J.* **2020**, *46*, 226–233. [[CrossRef](#)]

**Disclaimer/Publisher’s Note:** The statements, opinions and data contained in all publications are solely those of the individual author(s) and contributor(s) and not of MDPI and/or the editor(s). MDPI and/or the editor(s) disclaim responsibility for any injury to people or property resulting from any ideas, methods, instructions or products referred to in the content.